Coordinative Voltage Control Strategy with Multiple Resources for Distribution Systems of High PV Penetration

Preprint

Xiangqi Zhu and Yingchen Zhang
National Renewable Energy Laboratory

Presented at the 2018 World Conference on Photovoltaic Energy Conversion (WCPEC-7)
Waikoloa, Hawaii
June 10–15, 2018

NREL is a national laboratory of the U.S. Department of Energy
Office of Energy Efficiency & Renewable Energy
Operated by the Alliance for Sustainable Energy, LLC

This report is available at no cost from the National Renewable Energy Laboratory (NREL) at www.nrel.gov/publications.

Conference Paper
NREL/CP-5D00-71568
June 2018

Contract No. DE-AC36-08GO28308

NOTICE

This report is available at no cost from the National Renewable Energy Laboratory (NREL) at www.nrel.gov/publications.

Available electronically at SciTech Connect http:/www.osti.gov/scitech

Available for a processing fee to U.S. Department of Energy and its contractors, in paper, from:

U.S. Department of Energy
Office of Scientific and Technical Information
P.O. Box 62
Oak Ridge, TN 37831-0062
OSTI http://www.osti.gov
Phone: 865.576.8401
Fax: 865.576.5728
Email: reports@osti.gov

Available for sale to the public, in paper, from:

U.S. Department of Commerce
National Technical Information Service
5301 Shawnee Road
Alexandria, VA 22312
NTIS http://www.ntis.gov
Phone: 800.553.6847 or 703.605.6000
Fax: 703.605.6900
Email: orders@ntis.gov

Cover Photos by Dennis Schroeder: (left to right) NREL 26173, NREL 18302, NREL 19758, NREL 29642, NREL 19795.

NREL prints on paper that contains recycled content.

Coordinative Voltage Control Strategy with Multiple Resources for Distribution Systems of High PV Penetration

Xiangqi Zhu and Yingchen Zhang

National Renewable Energy Laboratory, Golden, Colorado, 80401, US

***Abstract* — This paper presents an optimal voltage control methodology with coordination among different voltage-regulating resources, including controllable loads, distributed energy resources such as energy storage and photovoltaics (PV), and utility voltage-regulating devices such as voltage regulators and capacitors. The proposed methodology could effectively tackle the overvoltage and voltage regulation device distortion problems brought by high penetrations of PV to improve grid operation reliability. A voltage-load sensitivity matrix and voltage-regulator sensitivity matrix are used to deploy the resources along the feeder to achieve the control objectives. Mixed-integer nonlinear programming is used to solve the formulated optimization control problem. The methodology has been tested on the IEEE 123-feeder test system, and the results demonstrate that the proposed approach could improve the voltage profile of distribution system operation.**

***Index Terms* — coordinative control, distribution system, high PV penetration, voltage control.**

NOMENCLATURE

C	Total cost of demand response ($)
i	Node number
j	Node number
M_{reg}	Total move of the regulators
M_{Tap}	Tap position of the regulator
n	Number of observable nodes in the system
n_T	Number of time steps in one power flow case
n_{reg}	Number of regulators
$P_{control}^{PV}(i)$	PV curtailment on node *i* (kW)
$P_{control}^{PV}\|_{max}(i)$	Maximum PV curtailment possible at node *i* (kW)
$P_{control}^{Load}(i)$	Response using controllable load at node *i* (kW)
$P_{control}^{Load}\|_{max}^{up}(i)$	Maximum load increases possible at node *i* (kW)
$P_{control}^{Load}\|_{max}^{down}(i)$	Maximum load decreases possible at node *i* (kW)
δP	Real power perturbation (kW)
p_{ij}	Sensitivity factor for real power
$Q_{control}^{PV}\|_{max}(i)$	Maximum possible reactive power support provided by smart inverter at node *i* (kvar)
$Q_{cap}(i)$	Capacity of the capacitor at node *i* (kvar)
q_{ij}	Sensitivity factor for reactive power
R_t^{Tap}	Tap coefficient of the regulator
r_{ij}	Sensitivity factor for regulators
$s(i)$	Status of on or off (1/0) of the capacitor at node *i*
t	Regulator number
$V^0(i)$	Voltage magnitude of each node at current time step (p.u.)
$V^1(i)$	New voltage after regulators move
$V_{\lim it}^{low}$	Lower bound of voltage limit (p.u.)
$V_{\lim it}^{high}$	Upper bound of voltage limit (p.u.)
ΔV	Total squared voltage deviation (p.u.^{2})
$\delta V(i)$	Voltage deviation at bus *i*
$VLSM_P$	VLSM of real power
$VLSM_Q$	VLSM of reactive power
Z	Minimization objective
λ_{PV}^P	Price of real power reduction at smart inverter ($/kW)
λ_{PV}^Q	Price of reactive power generation or absorption at smart inverter ($/kW)
λ_{cap}	Price of turning on the capacitor at node *i*, $/kvar
λ_{Load}	Price of demand response of controllable loads at node *i* ($/kW)
λ_{reg}	Price of regulator moves
$\omega_1, \omega_2, \omega_3$	Weight coefficient
ξ	Correction coefficient

I. INTRODUCTION

THE installed capacities of photovoltaic (PV) systems, including residential/commercial rooftop PV, and utility-scale PV power plants have been growing rapidly in recent years. High penetrations of PV can affect power system voltage, causing rapid voltage variations and large voltage ramps [1-5]. This can impact distribution system reliability and limit the further acceptance of distributed energy resources (DERs). Studies have shown that additional voltage regulation devices might be required in distribution systems or existing devices will need to act more frequently, potentially reducing of the lifetimes of those devices [6].

Existing studies focus on resolving voltage issues by revising settings for voltage regulation devices in distribution systems, including voltage regulators and capacitor banks [7]–[8]; however, only a few voltage regulation devices are installed on a distribution system, and their operation is limited by their locations. Devices such as capacitor banks and mechanically switched shunt devices do not have many levels of control. There are also proposals to use the fast response from power electronics interfaces of DERs, such as PV inverters, to regulate the voltage profiles of distribution systems. Although the performance of such control paths is promising, it is costly to install controllers and necessary communications for millions

of distribution devices [9]. The most feasible solution for utility companies will be to control existing legacy devices simultaneously with some power electronics-interfaced devices to greatly enhance performance while reducing cost.

In this paper, we propose coordinative voltage control at distribution feeders by coordinating demand response (DR), PV inverters, and utility legacy voltage controllers to regulate voltage. Controllable loads, PV, and capacitors are all considered as demand response resources because they could response to a kW or kvar dispatch command and alter the net load profile. Applying an effective control strategy to deploy demand response resources and coordinating with voltage regulators could address the voltage problems brought by high penetrations of PV.

In [10], a demand response approach applied in an automated distribution system for voltage control is proposed, but it focuses only on emergency events, such as outages of generators and lines. In [11], a method of aggregating small electric appliances to provide voltage regulation is proposed; however, only load was used as a demand response resource, and coordination among different resources—such as load, PV, capacitors, and voltage regulators—was not considered. The concept of a sensitivity coefficient of voltage was used in [11]; however, the authors assumed that the coefficient could be calculated using the information obtained by state estimation, and they calculated the coefficient at every time step. But state estimation is difficult in the distribution system because of the lack of measurements and calculating the coefficient at every time step increases computational overhead.

In this paper, a voltage load sensitivity matrix (VLSM) and voltage regulator sensitivity matrix (VRSM) have been developed and a voltage optimizer is designed with the objective to minimize voltage deviations, total cost, and voltage regulator moves while removing voltage violations. The VLSM and VRSM were pre-calculated; they do not need to be calculated at every time step, thus, the heavy computation load could be avoided.

The contributions of this paper are twofold. First, we developed a VLSM and VRSM-based control strategy that could effectively tackle the voltage problem and improve reliability of distribution systems with high penetrations of PV. Second, we account for coordination among different resources, including customer-owned and utility-owned devices.

The rest of this paper is organized as follows. Section II introduces the optimization control strategy. Section III discusses and analyzes the case studies. The summary and future work are presented in Section IV.

II. Control Strategy Modeling

This section first introduces the VLSM and VRSM and then presents the proposed control strategy formulation.

A. Voltage-Load Sensitivity Matrix (VLSM)

$VLSM_P$ and $VLSM_Q$ are defined as the sensitivity matrixes for real power and reactive power, respectively [12]. The voltage change, δV_i, at node i can be estimated by the real power change, δP_j, and the reactive power change, δQ_j, at all nodes (i.e., $j = 1 \ldots n$) using the *VLSM* as follows:

$$|\delta V| = |VLSM_P||\delta P| + |VLSM_Q||\delta Q| \quad (1)$$

i.e.,

$$\begin{vmatrix} \delta V(1) \\ \vdots \\ \delta V(n) \end{vmatrix} = \begin{vmatrix} p_{11} & \cdots & p_{1n} \\ \vdots & \ddots & \vdots \\ p_{n1} & \cdots & p_{nn} \end{vmatrix} \begin{vmatrix} \delta P(1) \\ \vdots \\ \delta P(n) \end{vmatrix} + \begin{vmatrix} q_{11} & \cdots & q_{1n} \\ \vdots & \ddots & \vdots \\ q_{n1} & \cdots & q_{nn} \end{vmatrix} \begin{vmatrix} \delta Q(1) \\ \vdots \\ \delta Q(n) \end{vmatrix} \quad (2)$$

From (2), we can derive:

$$\delta V(i) = \sum_{j=1}^{n} p_{ij}\, \delta P(j) + \sum_{j=1}^{n} q_{ij}\, \delta Q(j) \quad (3)$$

where p_{ij} and q_{ij} represent the real and reactive power sensitivity factors at bus *i* with respect to bus *j*.

The sensitivity factors represent the voltage change expected at bus *i* when there is one unit real and reactive power perturb at bus *j*.

The VLSM is obtained by calculating the voltage changes when perturbing real and reactive power at each load bus. For instance, $VLSM_P$ is calculated as following:

First, the base voltage matrix |*V0*| is obtained. The voltage profiles of the load buses are obtained by performing the feeder simulation using base load profiles, *Load0*. |*V0*| is constructed by putting the voltage profiles at the nodes into a matrix. If there are *n* load nodes and n_T time-series simulation steps in total, the dimension of the matrix will be $n \times n_T$.

Second, the perturbed voltage matrix |*V1*| is obtained. The load profile used at bus *i* is perturbed by adding a flexible number δ (either positive or negative) to obtain another load profile, *Load1*. Then the feeder simulation is done with *Load1* to obtain new voltage profiles at the nodes. Then, |*V1*| is obtained in a way similar to getting |*V0*|.

Third, column *i* of $VLSM_P$ is obtained. Matrix $|\delta V|$ is acquired by subtracting |*V1*| by |*V0*|. Then, column *i* of $VLSM_P$ is obtained by using the average value of each row in $|\delta V|$ divided by the perturbation δ.

Finally, $VLSM_P$ will be obtained by repeating these three steps for every bus.

B. Voltage-Regulator Sensitivity Matrix (VRSM)

As shown in (4), VRSM is defined as sensitivity matrix for regulators. r_{it} is defined as sensitivity factor of the i^{th} node to the t^{th} regulator. The new voltage $V^1(i)$ at node *i* could be calculated by (5). For better illustration, (5) is expanded to (6): first, the product of the sensitivity factor and the associated regulator tap coefficient for each node is summed, then the new voltage at each node is calculated by multiplying the old voltage by the summation results.

$$VRSM = \begin{vmatrix} r_{11} & \cdots & r_{1n_{reg}} \\ \vdots & \ddots & \vdots \\ r_{n1} & \cdots & r_{nn_{reg}} \end{vmatrix} \quad (4)$$

$$V^1(i) = V^0(i) \sum_{t=1}^{n_{reg}} R_t^{Tap} r_{it} \quad (5)$$

$$\begin{vmatrix} V^1(1) \\ V^1(2) \\ \vdots \\ V^1(n) \end{vmatrix} = \begin{vmatrix} V^0(1) * (R_1^{Tap} r_{11} + R_2^{Tap} r_{12} + \cdots R_{n_{reg}}^{Tap} r_{1n_{reg}}) \\ V^0(2) * (R_1^{Tap} r_{21} + R_2^{Tap} r_{22} + \cdots R_{n_{reg}}^{Tap} r_{2n_{reg}}) \\ \vdots \\ V^0(n) * (R_1^{Tap} r_{n1} + R_2^{Tap} r_{n2} + \cdots R_{n_{reg}}^{Tap} r_{nn_{reg}}) \end{vmatrix} \quad (6)$$

VRSM is also derived from the perturbation. Each regulator is made to move one step up and down in turns. Then the influence of the t^{th} regulator to the nodes will be quantified and form the t^{th} column of the VRSM.

C. Control Strategy Modeling

The overall optimization objective is to minimize the total cost, voltage deviations, and voltage regulator moves while eliminating voltage violations in the distribution system. The optimization problem is formulated in (7)–(19):

$$\text{Min} \quad Z = \omega_1 \xi_1 C + \omega_2 \Delta V + \omega_3 \xi_2 M_{reg} \quad (7)$$

$$C = \lambda_{Load} \sum_{i=1}^{n} \left(P_{control}^{Load}(i)\right)^2 + \lambda_{PV}^{P} \sum_{i=1}^{n} \left(P_{control}^{PV}(i)\right)^2 + \lambda_{PV}^{Q} \sum_{i=1}^{n} \left(Q_{control}^{PV}(i)\right)^2 + \lambda_{cap} \sum_{i=1}^{n} \left(s(i) Q_{cap}(i)\right)^2 + \lambda_{reg} \sum_{t=1}^{n_{reg}} \left(M_{Tap}(t) - 2\right)^2 \quad (8)$$

$$\Delta V = \sum_{i=1}^{n} \left(V(i) - V_{obj}\right)^2 \quad (9)$$

$$V(i) = V^1(i) + \sum_{j=1}^{n} \left(VLSM_P(i,j) \cdot \left(P_{control}^{Load}(j) - P_{control}^{PV}(j) \right) \right) + \sum_{j=1}^{n} \left(VLSM_Q(i,j) \cdot \left(Q_{control}^{PV}(j) + s(j) Q_{cap}(j) \right) \right) \quad (10)$$

$$V^1(i) = V^0(i) * \sum_{t=1}^{n_{reg}} \left(\left(M_{Tap}^0(t) + (M_{tap}(t) - 2) * \Delta_{Tap} \right) * VRSM(t,i) \right) \quad (11)$$

$$M_{reg} = \sum_{t=1}^{n_{reg}} \left(M_{Tap}(t) - 2 - M_{Tap}^0(t) \right)^2 \quad (12)$$

Subject to:

$$0 < \omega_1, \omega_2, \omega_3 < 1 \quad (13)$$

$$\omega_1 + \omega_2 + \omega_3 = 1 \quad (14)$$

$$-P_{control}^{PV}|_{max}(i) < P_{control}^{PV}(i) < 0 \quad (15)$$

$$P_{control}^{Load}|_{max}^{down}(i) < P_{control}^{Load}(i) < P_{control}^{Load}|_{max}^{up}(i) \quad (16)$$

$$-Q_{control}^{PV}|_{max}(i) < Q_{control}^{PV}(i) < Q_{control}^{PV}|_{max}(i) \quad (17)$$

$$V_{limit}^{low} < V(i) < V_{limit}^{high} \quad (18)$$

$$1 \le M_{Tap}(j) \le 3, \quad M_{Tap}(j) \in \mathrm{Z} \quad (19)$$

As shown in (7), each optimization target is associated with a weight factor, ω, which enables emphasizing different optimization targets according to different needs. For example, ω_2 could be increased much higher than ω_1 and ω_3 to minimize the voltage fluctuation at best effort. Because the absolute value of the C and M_{reg} are not the same, two correcting coefficients, ξ_1 and ξ_2, have been applied to balance the optimization objectives. As shown in (8), each voltage regulation resource is associated with a price, λ, so we could easily limit the use of one resource by raising the associated price. For example, we could limit PV providing voltage control by raising the PV control price λ_{PV}^{P} to limit curtailment. The voltage regulators are constrained to one step move at most in each control cycle.

As shown in (18), the voltage at each node of the feeder will be constrained in a defined range. The lower and upper bounds can be adjusted as needed. Usually the range will follow ANSI C84.1 as [0.95, 1.05].

III. Case Studies

Case studies will be discussed in this section. The test case presented here is performed on the IEEE 123-bus system, which is shown in Fig. 1. The voltage level is 4.16 kV. There are 91 load buses in the system. The peak load is 3,227 kW/1,625 kvar. The PV installation capacity is 3,125 kW. There are 4 capacitors installed, one each at nodes 83, 88, 90, and 92, with capacities of 200 kvar, 50 kvar, 50 kvar, and 50 kvar, respectively. Four regulators are installed: at the feeder head and nodes 9, 25, and 160, including three-phase regulators and single-phase regulators.

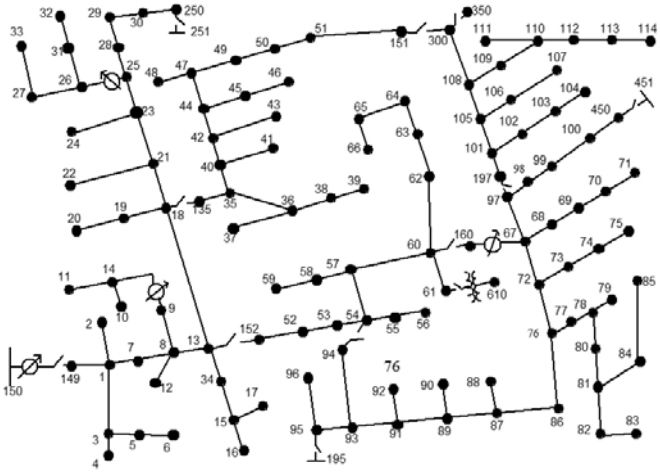

Fig. 1. Feeder topology of the IEEE 123-bus system.

Three case studies will be discussed in this section. First, details of the control result for one control cycle will be presented. Then, a 24-hour time-series study will be demonstrated to validate the stability of the proposed control methodology. In the third case, the price for the voltage regulator move will be adjusted to a lower level; in this way, the legacy devices control ability will be demonstrated.

A. Single Control Cycle Case

The results for the single control cycle are shown in Fig. 2. The demand response results and the voltage results are shown in Fig. 2 (a) and Fig. 2 (b), respectively. The x-axis of Fig. 2 (a) and Fig. (b) represent the nodes from 1st to 91st, the y-axis

represents the demand response amount (kW or kvar) and voltage magnitude, respectively. It could be observed from Fig. 2 (a) that demand response (the demand response in this context refers to net load change brought by both load and distributed PV) contributions from the PV smart inverter and load of each node have been deployed to regulate the voltage. In Fig.2 (b), V_{beforeDR} is the voltage magnitude before implementing the demand response; $V_{\text{afterDR-estimated}}$ is the estimated voltage magnitude calculated according to the VLSM and demand response optimization results; and $V_{\text{afterDR-actual}}$ is the actual voltage after the demand response deployment. As shown in this figure, the calculated voltage is very close to the actual voltage. This demonstrates that using VLSM to substitute the complex power flow calculation produces an unbiased result.

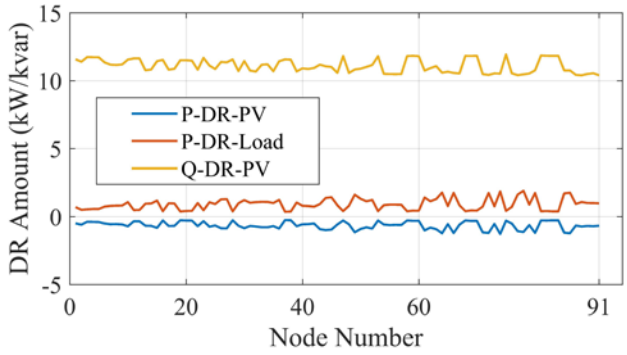

Fig.2(a). Demand response results for single control cycle.

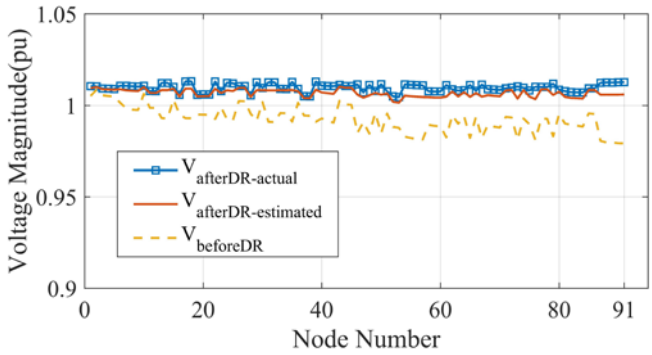

Fig.2(b). Voltage results for single control cycle.

B. *Twenty-Four-Hour Time-Series Case*

A 24-hour time-series study has been done to test the control strategy. The control is performed every 5 minutes, so we have 288 control steps for 1 day. The voltage profiles before and after performing the control strategy at a sample node are shown in Fig. 3. As shown, the voltage profiles after control are within the limits and do not have large fluctuations. Similar to Fig. 2, here the $V_{\text{afterDR-estimated}}$ is the estimated voltage magnitude calculated in GAMS by solving the formulated optimization problem presented in Section II; $V_{\text{afterDR-actual}}$ is the actual voltage from the simulation in OpenDSS after implementing the optimization results on the feeder model. The percentage error of the estimated voltage defined in (20) is used to estimate the accuracy of the VLSM estimated voltage.

$$Percentage\ Error = \frac{|V_{actual} - V_{estimated}|}{V_{actual}} \quad (20)$$

Considering all the nodes in the 123-feeder system, the maximum and minimum voltage magnitudes during this day are shown in Table I. As shown, they are all within the voltage limits. We performed 288 control steps for 91 nodes, so in total we have 26,208 cases to check the error rate statistics. The error rate statistics are shown in Table II; it can be observed that the error rate is very small: the maximum is 1%. To get rid of the complex power flow calculation and reduce the time of solving optimization problem, we use the VLSM and VRSM to calculate voltage in the optimization formulation. So, we need to make sure the VLSM and VRSM we calculated using the method presented in this paper will not cause large errors in all cases comparing to real power flow. The low error rate demonstrated the effectiveness of the VLSM and VRSM.

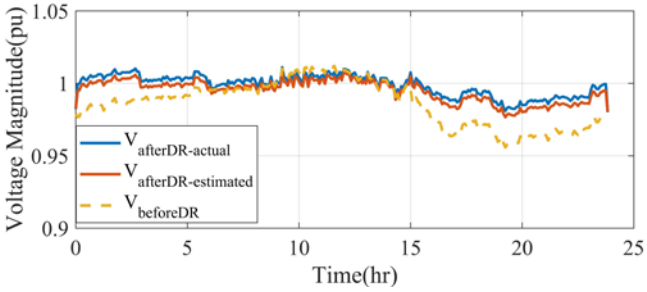

Fig. 3. Voltage profiles at Bus 37, Phase A.

TABLE I
VOLTAGE RANGE

Maximum voltage (p.u.)	Minimum voltage (p.u.)
1.0082	0.9766

TABLE II
ERROR PERCENTAGE FOR TIME-SERIES STUDY

Mean	Min	Median	Max
0.23%	8.26×10^{-6}%	0.28%	1%

C. *Voltage Regulator Case*

In this specific case, the cost of the voltage regulator move and the weight coefficient associated with the total voltage regulator move minimization have been adjusted to a lower level; therefore, the voltage regulator has been triggered to move for the voltage regulation.

As shown in Fig. 4 (a), $V_{\text{afterRegMove}}$ represents the voltages at the nodes after the corresponding regulators moved. Comparing $V_{\text{afterRegMove}}$ with V_{beforeDR}, it could be observed that the voltages have been improved after the regulator worked. In this case, two regulators moved: the three-phase voltage regulator on the feeder head and the single voltage regulator on Phase A of Node 160 both moved up one step to improve the voltage.

The two rows for the two regulators in the VRSM are plotted in Fig. 4 (b). The x-axis represents the node number, from 1–91; the y-axis represents the regulator effect on each node, where 1 represents that this regulator has influence on this node and 0 represents that this regulator does not affect this node.

The demand response deployment of load and the PV smart inverter from each node is shown in Fig. 4 (c). After the regulator worked, the demand resources needed will be less.

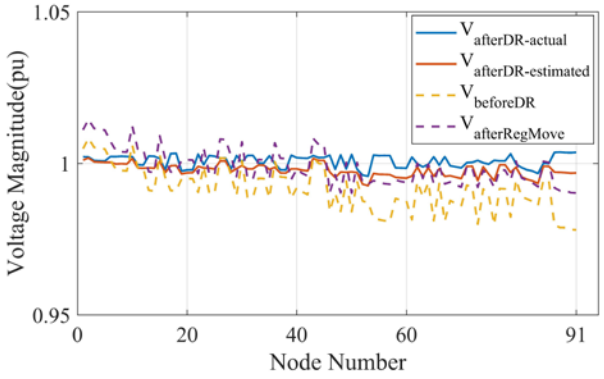

Fig. 4(a). Voltage results for voltage regulator case.

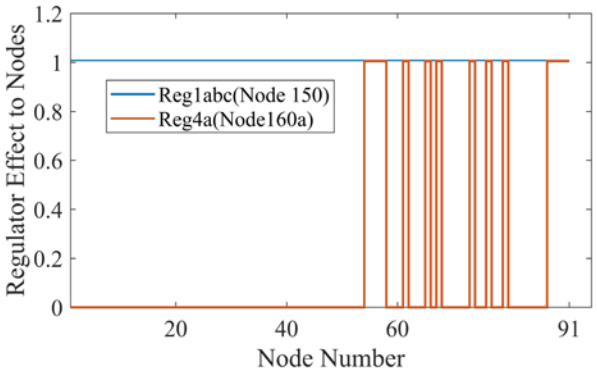

Fig. 4(b). Regulator influence on each node.

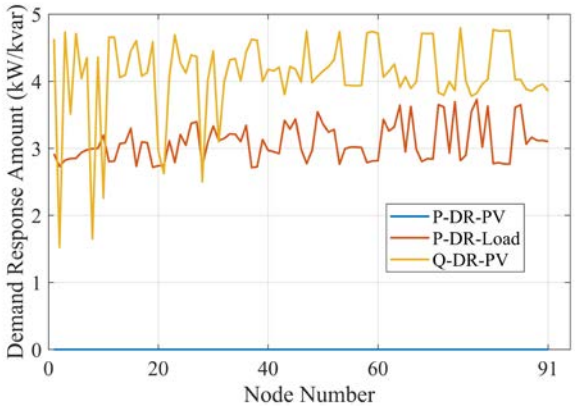

Fig. 4(c). Demand response results for voltage regulator case.

IV. Summary and Future Work

A coordinative voltage control strategy deploying different type of resources on a distribution system is developed in this paper to tackle the voltage problem, achieving a more reliable grid with PV integration.

The VLSM we developed enables us to consider coordination among different resources, including customer-owned and utility-owned devices, so that the voltage problem brought about by high penetrations of PV can be addressed.

We tested the control strategy on the IEEE 123-feeder test system, and the results demonstrated the effectiveness and capability of this control scheme. Our future work is to implement this control strategy on a realistic distribution system from a utility partner and perform case studies for multiple scenarios.

Acknowledgement

This work was authored by Alliance for Sustainable Energy, LLC, the manager and operator of the National Renewable Energy Laboratory for the U.S. Department of Energy (DOE) under Contract No. DE-AC36-08GO28308. Funding provided by U.S. Department of Energy Office of Energy Efficiency and Renewable Energy Solar Energy Technologies Office, ENERGISE Grid Optimization with Solar (GO-Solar) Project . The views expressed in the article do not necessarily represent the views of the DOE or the U.S. Government. The U.S. Government retains and the publisher, by accepting the article for publication, acknowledges that the U.S. Government retains a nonexclusive, paid-up, irrevocable, worldwide license to publish or reproduce the published form of this work, or allow others to do so, for U.S. Government purposes.

References

[1] D. Lew, N. Miller, K. Clark, G. Jordan, and Z. Gao, “Impact of high solar penetration in the western interconnection,” Nat. Renew. Energy Lab., Denver, CO, USA, Tech. Rep. NREL/TP-5500-49667, Dec. 2010.

[2] J. Bank, B. Mather, J. Keller, and M. Coddington, “High penetration photovoltaic case study report,” Nat. Renew. Energy Lab., Denver, CO, USA, Tech. Rep. NREL/TP-5500-54742, Jan. 2013.

[3] J. Wang, X. Zhu, D. L. Lubkeman, N. Lu, and N. Samaan, “Continuation Power Flow Analysis for PV Integration Studies at Distribution Feeders.” Innovative Smart Grid Technologies (ISGT), 2016 IEEE PES. IEEE, 2016.

[4] Liu, Y., Bebic, J., Kroposki, B., De Bedout, J., & Ren, W. (2008, November). Distribution system voltage performance analysis for high-penetration PV. In Energy 2030 Conference, 2008. ENERGY 2008. IEEE (pp. 1-8). IEEE.

[5] Ari, G. K., & Baghzouz, Y. (2011, June). Impact of high PV penetration on voltage regulation in electrical distribution systems. In Clean Electrical Power (ICCEP), 2011 International Conference on (pp. 744-748). IEEE.

[6] S. Lu, N. Samaan, D. Meng, F. Chassin, Y. Zhang, B. Vyakaranam, M. Warwick, J. Fuller, R. Diao, T. Nguyen, and C. Jin, “Duke Energy Photovoltaic Integration Study: Carolinas Service Areas.” No. PNNL-23226, Pacific Northwest National Laboratory (PNNL), Richland, WA, USA, 2014.

[7] M. E. Baran, H. Hooshyar, Z. Shen, and A. Huang, "Accommodating high PV penetration on distribution feeders." *IEEE Transactions on Smart Grid* vol. 3, no. 2, pp. 1039-1046, May 2012.

[8] P. Kundur, N. J. Balu, and M. G. Lauby, *Power System Stability and Control*, Vol. 7. New York: McGraw-Hill, 1994.

[9] Giordano, V., Gangale, F., Fulli, G., Jiménez, M. S., Onyeji, I., Colta, A., ... & Maschio, I. (2011). Smart grid projects in Europe. JRC Ref Rep Sy, 8.

[10] A. Zakariazadeh, O. Homaee, S. Jadid, and P. Siano. "A new approach for real time voltage control using demand response in an automated distribution system." *Applied Energy*, vol. 117, pp. 157-166, 15 March 2014.

[11] K. Christakou, D.-C. Tomozei, J.-Y. Le Boudec, and M. Paolone, "GECN: Primary voltage control for active distribution networks via real-time demand-response." *IEEE Transactions on Smart Grid*, vol. 5, no.2, pp. 622-631, Sept. 2014

[12] X. Zhu, J. Wang, D. Lubkeman, N. Lu, N. Samaan, and R. Huang. "Voltage-load sensitivity matrix based demand response for voltage control in high solar penetration distribution feeders," Power and Energy Society General Meeting (PESGM), 2017. IEEE, 2017.